JBC RESEARCH ARTICLE

Protein acetylation-mediated cross regulation of acetic acid and ethanol synthesis in the gas-fermenting *Clostridium ljungdahlii*

Received for publication, August 14, 2021, and in revised form, December 16, 2021 Published, Papers in Press, December 24, 2021,
https://doi.org/10.1016/j.jbc.2021.101538

Yanqiang Liu[1,2], **Ziwen Zhang**[1,2], **Weihong Jiang**[1,*], **and Yang Gu**[1,*]

From the [1]*Key Laboratory of Synthetic Biology, The State Key Laboratory of Plant Carbon-Nitrogen Assimilation, CAS Center for Excellence in Molecular Plant Sciences, Shanghai Institute of Plant Physiology and Ecology, Chinese Academy of Sciences, Shanghai, China;* [2]*University of Chinese Academy of Sciences, Beijing, China*

Edited by Chris Whitfield

The autotrophic acetogen *Clostridium ljungdahlii* has emerged as a major candidate in the biological conversion of one-carbon gases (CO_2/CO) to bulk chemicals and fuels. Nevertheless, the regulatory pathways and downstream metabolic changes responsible for product formation and distribution in this bacterium remain minimally explored. Protein lysine acetylation (PLA), a prevalent posttranslational modification, controls numerous crucial cellular functions. Herein, we revealed a novel cross-regulatory mechanism that uses both the PLA system and transcription factors to regulate the carbon flow distribution for product formation in *C. ljungdahlii*. The dominant acetylation/deacetylation system (At2/Dat1) in *C. ljungdahlii* was found to regulate the ratio of two major products, acetic acid and ethanol. Subsequent genetic and biochemical analyses revealed that the activities of Pta and AdhE1, two crucial enzymes responsible for acetic acid and ethanol synthesis, respectively, were greatly affected by their levels of PLA. We found that the acetylation statuses of Pta and AdhE1 underwent significant dynamic changes during the fermentation process, leading to differential synthesis of acetic acid and ethanol. Furthermore, the crucial redox-sensing protein Rex was shown to be regulated by PLA, which subsequently altered its transcriptional regulation on genes responsible for acetic acid and ethanol formation and distribution. Based on our understanding of this cross-regulatory module, we optimized the ethanol synthetic pathway by modifying the acetylation status (deacetylation-mimicked mutations of crucial lysine residues) of the related key enzyme, achieving significantly increased titer and yield of ethanol, an important chemical and fuel, by *C. ljungdahlii* in gas fermentation.

Autotrophic acetogens can use the reductive acetyl-CoA pathway for the production of acetic acid and ethanol as well as some other minor metabolites such as butanol, lactate, butyrate, hexanoate, and 2,3-butanediol using CO_2 and CO as the carbon sources (1). Some acetogens are human gut bacteria that are closely associated with human intestinal health (2). The fermentation process of autotrophic acetogens typically proceeds in two phases, acidogenesis and alcohologenesis, during which acetic acid and ethanol accumulate as the major products (3). Such a biphasic physiological process is an essential characteristic of these anaerobes. With the increasing interest in the biological usage of C1 gases, the detailed investigation of the biphasic metabolism of autotrophic acetogens has become a research focus.

Our current knowledge includes an understanding of the metabolic pathways responsible for the formation of acids and alcohols as well as of the conversion of acids to alcohols in autotrophic acetogens (1, 4–7). Furthermore, some key enzymes and the corresponding genes have been identified and characterized (5). In contrast, the regulatory aspects of the distinctive metabolism of these autotrophic acetogens still remain largely unknown. Some external environmental factors have been reported to affect the acid and alcohol synthesis of autotrophic acetogens. For example, low temperature and some metal ions (Ni^{2+}, Co^{2+}, etc.) could enable *Clostridium carboxidivorans* P7 to produce more ethanol (8, 9); W^{6+} could help *Sporomusa ovata* to produce more ethanol (10); and the addition of some amino acids such as arginine in media could reduce the accumulation of acetic acid by boosting the ATP level in *Clostridium autoethanogenum* (11). However, the molecular mechanisms underlying these findings are unclear. Obviously, to develop an efficient gas fermentation process, a detailed understanding of the regulatory mechanism of the metabolic processes in these autotrophic acetogens is indispensable.

Protein Lysine acetylation (PLA) is known to be a crucial metabolic regulatory mechanism in both prokaryotic and eukaryotic cells, in which multiple PLA-regulated physiological and metabolic processes have been revealed (12–14). In a previous study on *Clostridium ljungdahlii*, a representative autotrophic acetogen, we revealed an interactive regulation module that uses both the global transcriptional factor CcpA and acetylation/deacetylation system At2/Dat1 to control carbon fixation (15). This finding suggested that, in addition to TFs, PLA plays an important role in regulating crucial cellular functions in autotrophic acetogens, leading to the regulation

* For correspondence: Yang Gu, ygu@cemps.ac.cn; Weihong Jiang, wjiang@cemps.ac.cn.

on several levels involving multiple factors. Despite of the importance of PLA in metabolic regulation, studies regarding the PLA-mediated regulations remain focused on zymoproteins, and only very few regulatory proteins have been reported to be affected by PLA and consequently exhibited changed functions (15–17). Specific to autotrophic acetogen, whether and how the PLA statuses of regulatory proteins will affect crucial cellular performances, including growth and product synthesis, remain hardly explored. Unraveling more such regulatory mechanisms will facilitate our understanding of these important bacterial species.

Herein, we discovered the influence of the *in vivo* PLA levels on the product synthesis pattern in *C. ljungdahlii*. Through the following genetic and biochemical experiments, a multilevel regulatory module that uses both the lysine acetylation and transcriptional regulation systems to control product synthesis in *C. ljungdahlii* was revealed. Based on this concept, a metabolic engineering strategy involving the optimization of both the expression and acetylation levels of the pathway genes was adopted to alter the product synthesis pattern in *C. ljungdahlii*, achieving a much higher yield and ratio of ethanol in gas fermentation.

Results

The product synthesis pattern in C. ljungdahlii *was regulated by the global protein acetylation level*

C. ljungdahlii yields two dominant products, acetic acid and ethanol, in gas fermentation. The crucial genes responsible for the synthesis of these two chemicals include *pta* (coding for phosphate acetyltransferase, CLJU_c12770), *ack* (coding for acetate kinase, CLJU_c12780), *adhE1/2* (coding for bifunctional alcohol and aldehyde dehydrogenase, CLJU_c16510/CLJU_c16520), and *aor1/2* (coding for aldehyde:ferredoxin oxidoreductase, CLJU_c20110/CLJU_c20210) (Fig. 1*A*). We examined the PLA status of the enzymes encoded by these six genes during gas fermentation based on our previous data (15). Notably, the Pta, Ack, and AdhE1/2 proteins were all acetylated at multiple lysine residues, whereas no acetylated lysine residue was found in Aor1/2 (15), indicating a potential influence of PLA on the activities of the former four enzymes (Fig. 1*B*).

To test the influence of the global protein acetylation level of *C. ljungdahlii* on product formation, a *C. ljungdahlii* mutant (Δ*dat1*) with deletion of the *dat1* gene (CLJU_c01320), which codes for the key deacetylase Dat1 in *C. ljungdahlii* (15), was used to examine product synthesis compared with that of the WT strain by fermenting syngas (a mixture of CO–CO_2–H_2–N_2). The results showed that the mutant and WT strains exhibited quite different selectivity toward the synthesis of acetic acid and ethanol, although they had similar growth properties (Fig. 1*C*). The obviously increased ethanol production, along with the decreased acetic acid production, was observed in the Δ*dat1* strain compared with the WT strain (Fig. 1*C*). Furthermore, the final titer of the total solvents (acetic acid and ethanol) of the Δ*dat1* strain was approximately 10% higher than that of the control strain (Fig. 1*C*). Such phenotypic changes of the Δ*dat1* strain could be recovered by reintroducing the *dat1* gene (Fig. 1*D*). These findings suggest that PLA plays a role in the regulation of the carbon flux distribution in *C. ljungdahlii*, resulting in changed product selectivity in gas fermentation.

The activities of key enzymes Pta and AdhE1 were greatly influenced by PLA

To explore if certain pathway genes and their PLA status are crucial for product formation in *C. ljungdahlii*, the mutants with deletion of each of the aforementioned six genes (*pta*, *ack*, *adhE1/2*, and *aor1/2*) were generated (Fig. S1 and Table S2) and then used to compare their performance with that of the WT strain in gas fermentation. The results showed that the Δ*pta*, Δ*ack*, and Δ*aor2* mutants grew much worse than the WT strain, and simultaneously, the Δ*adhE1* mutant exhibited greatly impaired ethanol production (Fig. S2, *A*–*C*, and *F*). In contrast, no obvious phenotypic changes were observed for the Δ*adhE2* and Δ*aor1* mutants (Fig. S2, *D* and *E*). These data suggested that *pta*, *ack*, *aor2*, and *adhE1* are crucial to the growth and product synthesis of *C. ljungdahlii* in gas fermentation.

Based on these findings, we further investigated whether PLA affects the activities of the Pta, Ack, Aor2, and AdhE1 enzymes. The purified Pta, Ack, Aor2, and AdhE1 proteins were separately treated *in vitro* by the purified acetyltransferase At2. A significantly increased acetylation level was observed for all these enzymes after the *in vitro* acetylation by At2 (Fig. 2*A*). The following assays showed that the increased acetylation level led to significant loss in the activities of Pta (56.6% loss) and AdhE1 (35.4% and 18.9% loss for its aldehyde dehydrogenase and alcohol dehydrogenase activity, respectively) (Fig. 2, *B* and *C*), whereas no obvious change was detected for Ack and Aor2 (Fig. 2, *D* and *E*). These results roughly revealed the causal relationships between the increased acetylation levels and decreased activities of these enzymes, although the impact of lysine acetylation on these enzyme activities may vary based on the efficiency of the *in vitro* acetylase treatment. Pta and AdhE1 are crucial for acetic acid and ethanol formation in *C. ljungdahlii* (Fig. 1*A*); therefore, the PLA-mediated regulation of these two enzymes may affect the carbon flux distribution between the synthetic pathways of acetic acid and ethanol, thereby altering the ratio of these two products.

However, we noticed that the decreased activities of Pta and AdhE1 caused by their increased acetylation levels cannot explain the greatly increased ethanol production of *C. ljungdahlii* after *dat1* deletion (Fig. 1*C*). It seems that PLA can control the product synthesis *via* other approaches in *C. ljungdahlii*.

The At2-mediated acetylation of the redox-sensing protein Rex greatly influenced product synthesis in gas fermentation

An examination of the results obtained from our previous acetylproteomic analyses of *C. ljungdahlii* suggested that a great number of TFs were acetylated at multiple lysine residues (15), indicating that the regulatory activities of these TFs may

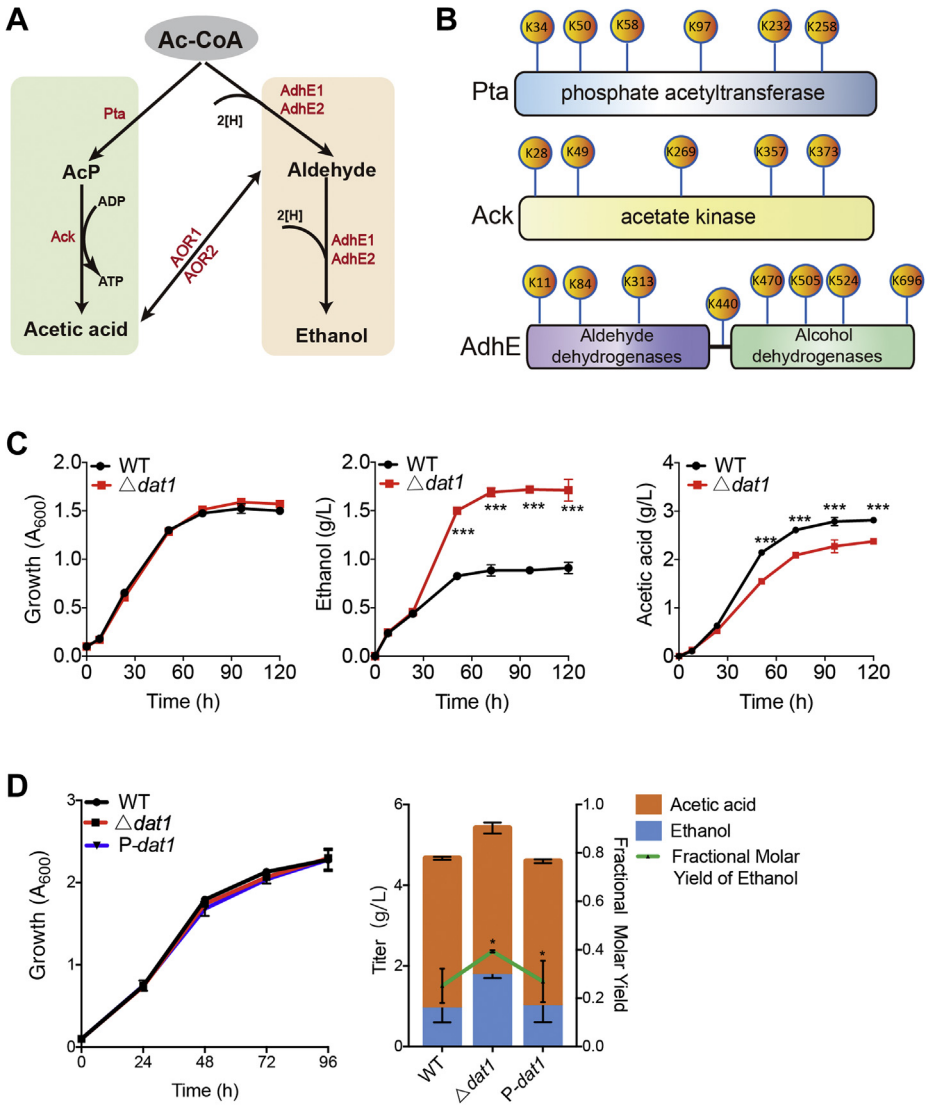

Figure 1. Lysine acetylation differentially influences acetic acid and ethanol synthesis in *Clostridium ljungdahlii*. *A*, schematic diagram of acetic acid and ethanol production as well as their conversion in *C. ljungdahlii*. *B*, acetylated lysine residues on Pta, Ack, and AdhE. Here, the acetylated lysine residues of AdhE include those from both AdhE1 and AdhE2, because these two proteins show very high amino acid sequence identity (87.36%) and their fragmented peptides containing acetylated lysine residues could not be distinguished by mass spectrometry data. *C*, comparison of the growth and ethanol and acetic acid production of the WT and Δ*dat1 C. ljungdahlii* strains in gas fermentation. *D*, growth (*left*) and product formation (*right*) of the WT, Δ*dat1*, and complemented strains. The complemented strain was obtained by the transformation of a plasmid expressing the *dat1* gene. The data are presented as mean ± SD (error bars; n = 3). Statistical analysis was performed using a two-tailed Student's *t* test. ***$p < 0.001$; *$p < 0.05$. Ack, acetate kinase; AdhE1/2, bifunctional alcohol and aldehyde dehydrogenase; Aor1/2, aldehyde:ferredoxin oxidoreductase; Pta, phosphotransacetylase.

be affected by their PLA statuses. Furthermore, we found that many crucial genes (*pta-ack*, *adhE1*, and *aor2*) responsible for product formation showed significant changes in transcription at 24 and 48 h, early and middle period of exponential growth, respectively, after Δ*dat1* deletion (Fig. 3*A*). All these findings suggest that PLA may affect the product synthesis of *C. ljungdahlii via* regulating the acetylation level of related TFs.

Therefore, we examined all the highly acetylated TFs in *C. ljungdahlii* (Table S1) (15). Fortunately, two candidates, which are highly homologous to the *Clostridium acetobutylicum* ATCC 824 Rex (75.24% identity, 98% coverage, e-value 1e−124) and AbrB (92.59% identity, 100% coverage, e-value 5e−57) that are known to control product synthesis (18, 19), were found. Subsequently, these two proteins (named *Clj*Rex and *Clj*AbrB) were purified for the *in vitro* EMSAs, aiming to examine if they can directly act on the aforementioned pathway genes, including *adhE1*, *aor2*, and *pta-ack*. The results showed that *Clj*Rex could bind to the promoter regions of *adhE1*, *aor2*, and *pta-ack* (Fig. 3*B*), whereas *Clj*AbrB only recognized the first two (Fig. S3*A*). Next, more experiments were conducted to confirm whether PLA affects the regulatory activities of *Clj*Rex and *Clj*AbrB. These two TFs were separately treated *in vitro* by the purified acetyltransferase At2, yielding the At2-acetylated *Clj*Rex and *Clj*AbrB for EMSAs. Using the promoter regions of *adhE1*, *aor2*, and *pta-ack* as the DNA probes, no evident mobility shifts were observed for the At2-treated *Clj*Rex (*Clj*Rex^{At}) at any protein concentration

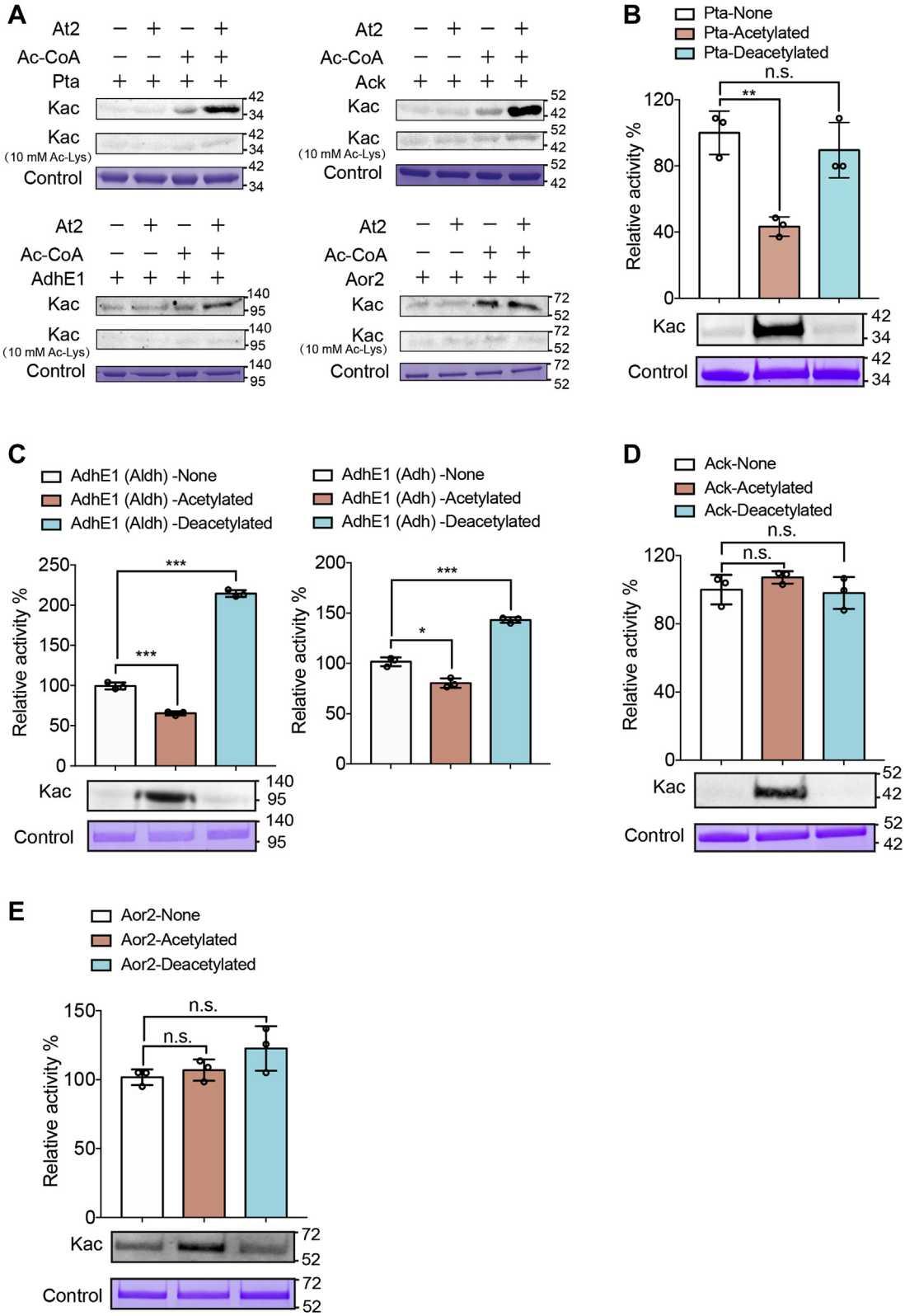

Figure 2. Regulation of the activities of Pta, Ack, AdhE1, and Aor2 by At2/Dat1-mediated lysine acetylation. *A*, influence of the At2 treatment on the acetylation levels of the purified Pta, Ack, AdhE1, and Aor2 proteins. The molecular weight markers were displayed on the *right* of the *boxes*. A significantly increased acetylation level was observed for all these enzymes after the *in vitro* acetylation by At2. All the data were representative of at least two independent experiments. 10 mM of free acetylated lysine (Ac-Lys) was used to outcompete the antiacetylated lysine antibodies during the Western blotting analysis, aiming to ensure that the Kac signal is because of the acetylation of lysine residues. (*B–E*, respectively) influence of the At2 or Dat1 (deacetylase) treatment on the activities of Pta, AdhE1 (a bifunctional enzyme that has the Aldh (aldehyde dehydrogenase) and Adh (alcohol dehydrogenase) activities), Ack, and Aor2. His-tagged Pta, Ack, AdhE1, and Aor2 were expressed in *Escherichia coli* and then purified for *in vitro* acetylation by At2 or deacetylation by Dat1. The error bars indicate SDs of triplicate measurements. The data are presented as mean ± SD (error bars; n = 3). Statistical analysis was performed using a two-tailed Student's *t* test. ***$p < 0.001$; **$p < 0.01$; *$p < 0.05$. n.s.: no significance. Ack, acetate kinase; AdhE1/2, bifunctional alcohol and aldehyde dehydrogenase; Aor1/2, aldehyde:ferredoxin oxidoreductase; Kac, lysine acetylation; Pta, phosphotransacetylase.

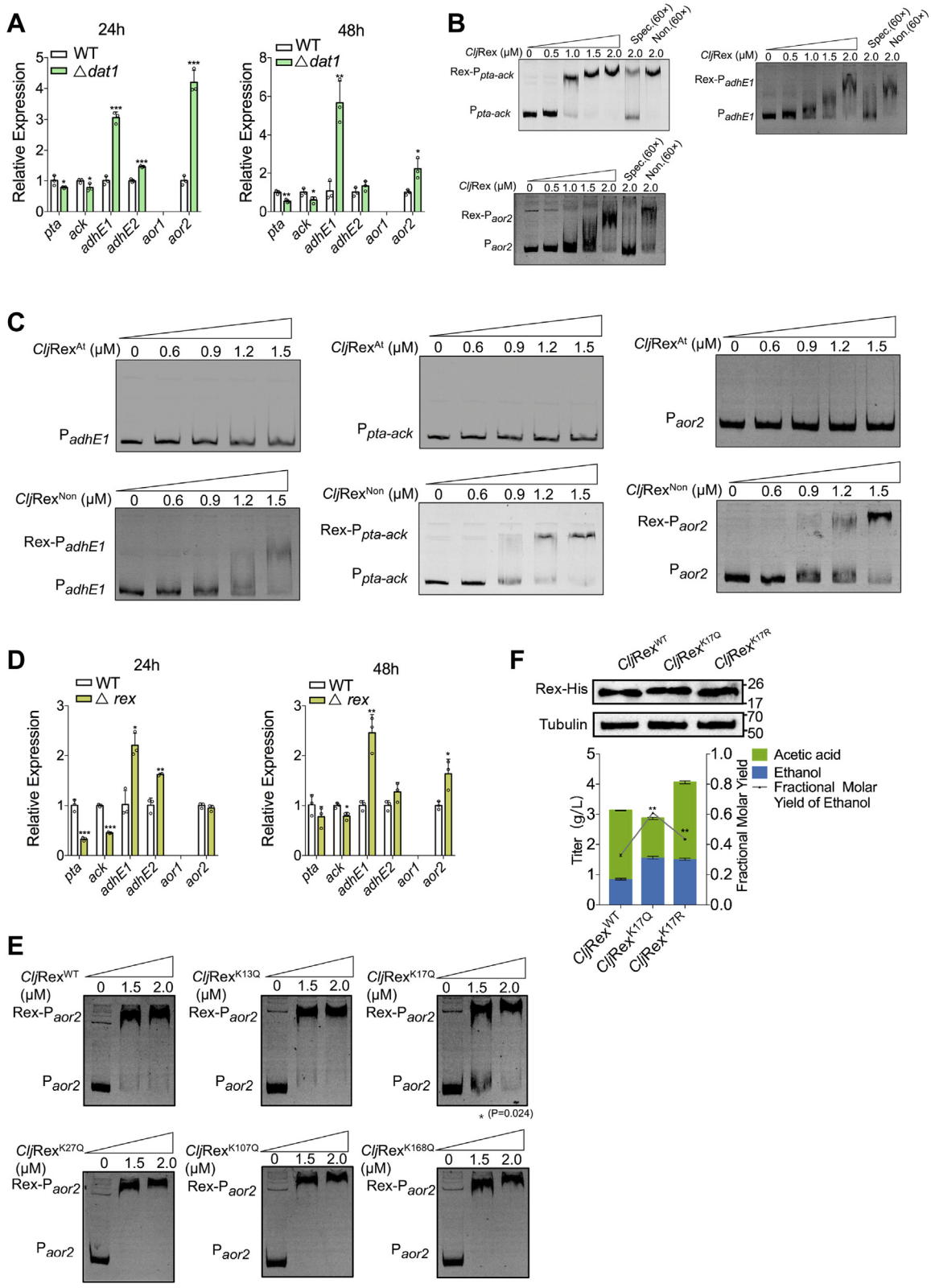

Figure 3. Effect of acetylation on the transcription factor Rex. *A*, transcriptional changes of the genes located in product synthetic pathways after *dat1* deletion in *Clostridium ljungdahlii*. *B*, confirmation of the binding activity of Rex to the promoters of the *adhE1*, *aor2*, and *pta-ack* genes. *Clj*Rex could bind to the promoter regions of *adhE1*, *aor2*, and *pta-ack*. *C*, binding of the *Clj*Rex^{Non} (without At2 treatment) and *Clj*Rex^{At} (*in vitro* At2 treatment) to the promoters of the *adhE1*, *aor2*, and *pta-ack* genes. No evident mobility shifts were observed for the At2-treated *Clj*Rex (*Clj*Rex^{At}) at any protein concentration; in contrast, evident mobility shifts were detected for *Clj*Rex^{Non} (without At2 treatment) using the same DNA probes. *D*, transcriptional changes of the genes located in product synthetic pathways after *rex* disruption in *C. ljungdahlii*. *E*, influence of acetylation-mimicking mutations on Rex–DNA-binding activity. The promoter of the *aor2* gene was used as the DNA probe. The K17Q mutation led to a much weaker *Clj*Rex binding to the DNA probe. *F*, influence of acetylation- and deacetylation-mimicking mutations (at the K17 residue) on acetic acid and ethanol formation. The plasmids expressing the original *rex*

(Fig. 3*C*); in contrast, evident mobility shifts were detected for *Clj*Rex^{Non} (without At2 treatment) using the same DNA probes (Fig. 3*C*). However, no obvious change was observed for the binding activity of *Clj*AbrB to the promoter regions of *adhE1* and *aor2* after At2 treatment (Fig. S3*B*). These findings suggest that the acetylation level could significantly affect the DNA-binding activity of *Clj*Rex to its target DNA fragments.

Therefore, we focused on *Clj*Rex and further analyzed its function in *C. ljungdahlii*. The *Clj*Rex coding gene *rex* (CLJU_c37250) was deleted (Fig. S1), yielding a mutant strain to examine the transcriptional changes of the genes located in the acetic acid and ethanol synthetic pathways. The results showed that, after *rex* deletion, the expressions of *adhE1* and *adhE2* (ethanol synthetic pathway) were up-regulated at 24 h, whereas those of *pta* and *ack* (acetic acid synthetic pathway) were significantly down-regulated at this timepoint (Fig. 3*D*); at 48 h, *adhE1* and *aor2* (acetic acid reassimilation) still showed obviously enhanced expressional levels compared to those of the WT strain (Fig. 3*D*). These data, combined with the EMSA results (Fig. 3*C*), suggest the direct regulation of *Clj*Rex on the genes located in product synthetic pathways in *C. ljungdahlii*.

The acetylproteome data revealed that *Clj*Rex contains five acetylation sites (Figs. S4 and S7; Table S5). We next sought to identify the key acetylation lysine residues that determine the regulatory function of *Clj*Rex. Thus, acetylation-mimicking mutations (K→Q) were introduced at these lysine residues, yielding five variants for DNA-binding activity analysis. As is shown in Figure 3*E* and Fig. S5, the K17Q mutation led to a much weaker *Clj*Rex binding to the DNA probe (the promoter region of the *aor2* gene), indicating the potential importance of acetylation at this lysine residue for the DNA-binding activity of *Clj*Rex. To further test whether the K17Q mutation at this residue could change the regulatory activity of *Clj*Rex *in vivo*, the original *Clj*Rex protein (*Clj*Rex^{WT}) and its two variants, that is, *Clj*Rex^{K17Q} and *Clj*Rex^{K17R} (acetylation- and deacetylation-mimicking mutation at K17, respectively), were separately introduced into the *rex*-deleted strain to examine their influence on product synthesis. The results showed that the expression of *Clj*Rex^{WT} and *Clj*Rex^{K17R} both led to the increase of the acetic acid titer and acetic acid/ethanol ratio compared to that of *Clj*Rex^{K17Q}, when the *in vivo* abundance of these three proteins were at a similar level (Fig. 3*F*). These data further verify the importance of the K17 residue for the *in vivo* function of *Clj*Rex in *C. ljungdahlii*.

Dynamic changes of the acetylation levels of Pta, AdhE1, and Rex in gas fermentation

Protein acetylation is a dynamic and reversible post-translational modification process. As we have revealed that the *in vitro* acetylation treatment affected remarkably the enzymatic activities of Pta and AdhE1 as well as the regulatory activity of *Clj*Rex (Figs. 2, *B* and *C* and 3*C*), how do their acetylation levels change during the entire fermentation process? To answer this question, we examined the dynamic changes of the acetylation levels of these three proteins in gas fermentation. Three plasmids that expressed the His-tagged Pta, AdhE1, and Rex proteins were introduced into the *C. ljungdahlii* mutants with the deletion of *pta*, *adhE1*, and *rex* (Fig. S1), respectively. The three yielding strains were cultivated using syngas and then, the grown cells at different stages (M, early logarithmic phase; L, late logarithmic phase; and S, stable growth phase) were collected for the protein purification of Pta, AdhE1, and Rex, which were further used for Western blot analysis. As is shown in Figure 4*A*, the acetylation levels of Pta were relatively low at all the three phases but slightly increased with the extension of fermentation; in contrast, AdhE1 exhibited a remarkably enhanced acetylation level at the S phase with the low acetylation levels at E and L stages. It is known that the WT *C. ljungdahlii* normally produces much less ethanol than acetic acid in gas fermentation (20); the significantly increased AdhE1 acetylation level and the resulting low AdhE1 activity in the latter fermentation stage (S stage) (Fig. 4*B*) may lead to the production of less ethanol at this stage than the earlier stages of fermentation.

The acetylation levels of *Clj*Rex gradually increased with the extension of fermentation (Fig. 4*C*), indicating a gradually decreased regulatory activity of *Clj*Rex. Given the differential regulation of *Clj*Rex on *adhE1*, *aor2*, and *pta-ack* (Fig. 3*D*), the dynamically changed *Clj*Rex acetylation level may affect the carbon flux distribution between the synthesis of acetic acid and ethanol; in the early phase, the relatively low acetylation level enables *Clj*Rex to efficiently activate the expression of *pta-ack* and repress the expression of *adhE1* and *aor2*, thereby contributing to acidogenesis at this stage; with the increase in *Clj*Rex acetylation, its regulatory strength toward *adhE1*, *aor2*, and *pta-ack* will decrease, alleviating the transcriptional repression on *adhE1* and *aor2* and subsequently leading to more ethanol production.

Improved product synthesis pattern of C. ljungdahlii *by modifying the acetylation status of key enzyme*

Acetic acid, rather than ethanol, is a dominant product in clostridial gas fermentation. Considering the importance of ethanol as the biofuel, we attempted to achieve a higher ethanol production and ethanol/acetic acid ratio by the specific elimination of the impact of acetylation on the activity of AdhE1 (the key enzyme located in ethanol synthetic pathway) *via* deacetylation-mimicking mutations (Fig. 5*A*).

First, to identify the acetylation sites of AdhE1, it was purified for *in vitro* acetylation by At2 and then detected for the acetylation sites by LC-MS/MS. The result (IPX0003486000),

gene and the Rex^{K17Q} and Rex^{K17R} encoding genes were separately introduced into the *C. ljungdahlii* mutant with the chromosomal deletion of *rex*. To measure the *in vivo* abundance of *Clj*Rex^{WT}, *Clj*Rex^{K17Q}, and *Clj*Rex^{K17R}, a 6xHis tag was inserted at the C-terminal of the corresponding genes on the expression plasmids for protein production in cells. The cell lysates were then used for Western blot analysis with the anti-His antibody. All data for the EMSA analyses (*B*, *C*, and *E*) were representative of at least two independent experiments. ***$p < 0.001$; **$p < 0.01$; *$p < 0.05$. Ack, acetate kinase; AdhE1/2, bifunctional alcohol and aldehyde dehydrogenase; Aor1/2, aldehyde:ferredoxin oxidoreductase; Pta, phosphotransacetylase.

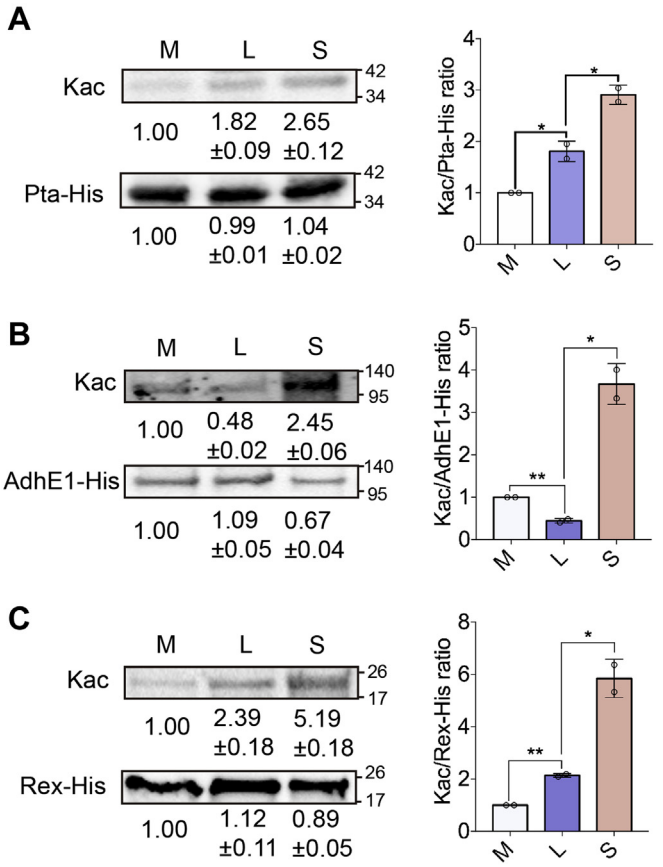

Figure 4. Dynamically changed acetylation levels of Pta, AdhE1, and Rex. *A*, acetylation levels of Pta at middle-(M), late-exponential (L), and stationary (S) stages. His-tagged Pta protein was expressed in the *Clostridium ljungdahlii* Δ*pta* strain grown in 1754 medium. The purified Pta protein was analyzed by Western blot using either anti-His or anti-AcK antibodies. The *right figure* shows the relative ratio of Pta acetylation *versus* Pta-His. The acetylation ratios of Pta at the L and S stages were calculated by comparing them with the M stage ratio, which was set to 1.00. *B* and *C*, acetylation levels of AdhE1 and Rex at different stages. The experimental details were the same as those for Pta. The data are presented as mean ± SD (error bars; n = 2). Statistical analysis was performed using a two-tailed Student's *t* test. $^{**}p < 0.01$; $^{*}p < 0.05$. Ack, acetate kinase; AdhE1/2, bifunctional alcohol and aldehyde dehydrogenase; Kac, lysine acetylation; Pta, phosphotransacetylase.

combined with our acetylproteome data (IPX0003487000 and IPX0003648000), a total of 11 acetylation lysine residues were found in AdhE1 (Figs. 5*B* and S8; Table S5). Next, acetylation-mimicking mutations (K→Q) were introduced at these 11 lysine residues separately, generating different AdhE1 variants for the identification of potential key acetylation lysine residues that determine the activity of AdhE1. As shown in Figure 5*C*, the 11 mutated *adhE1* genes were transformed into the *C. ljungdahlii* Δ*adhE1/2* strain for expression (Table S2), and the results showed that the K129Q, K379Q, K388Q, and K440Q mutations led to significant loss in ethanol production at 48 h. Subsequently, deacetylation-mimicking mutations (K→R) were introduced at these four sites; the results showed that the K129R mutant greatly impaired ethanol formation, whereas no obvious changes were found for the other three mutations (Fig. 5*C*). All these data indicate that the acetylation status of the K379, K388, and K440 sites are crucial for the *in vivo* AdhE1 activity; simultaneously, K129 is also a crucial amino acid residue for the *in vivo* AdhE1 activity, which, however, should not be associated with its acetylation status.

After identifying the three crucial lysine acetylation sites on AdhE1, the aforementioned metabolic engineering strategy was carried out. Using the Δ*dat1* strain (higher ethanol production and ethanol/acetic acid ratio against the WT strain) as a chassis (Fig. 1*C*), a plasmid that contained a mutated *adhE1* gene encoding AdhE1$^{K379/388/440R}$ (triple deacetylation-mimicked mutations at the K379, K388, and K440 sites) was constructed and introduced into the chassis for overexpression (Fig. 5*A*). Simultaneously, the *aor2* gene responsible for acetic acid reassimilation in *C. ljungdahlii* was also overexpressed (Fig. 5*A*). Here, the promoter used to drive gene expression was P_{pta}, obtained from the upstream noncoding region of the CLJU_c12770 gene that was upregulated in the presence of Rex (Fig. 3*D*). Notably, the cells expressing both *aor2* and the AdhE1$^{K379/388/440R}$ encoding gene (*adhE1*^{3M}) exhibited obviously increased ethanol and decreased acetic acid titers compared to the control strains (harboring the empty plasmid or the plasmid expressing *aor2* and *adhE1*) in gas fermentation (Fig. 5*D*), leading to a much higher ethanol/acetic acid ratio (Fig. 5*D*).

To further explore the fermentation potential of the engineered strain (*aor2* and *adhE1*^{3M}), $CaCO_3$ (0.1% w/v) was added into the medium for a rough control of pH. Using this modified medium, the engineered strain (*aor2* and *adhE1*^{3M}) was able to produce 4.72 ± 0.27 g/l of ethanol and 3.12 ± 0.13 g/l of acetic acid, whereas the WT strain produced 1.75 ± 0.06 g/l of ethanol and 4.07 ± 0.32 g/l of acetic acid (Fig. 5*E*). Therefore, a much higher total product titer (ethanol plus acetic acid) and ethanol/acetic acid ratio were achieved by the engineered strain. These results confirmed that the *in vivo* activities of the enzymes responsible for product synthesis in *C. ljungdahlii* could be effectively enhanced by eliminating the negative influence from lysine acetylation, thereby improving the titer of target products.

Discussion

In this study, we reported a complex regulatory mechanism, which is mediated by both the redox-sensing protein Rex and the PLA system for the regulation of product synthesis in the autotrophic acetogen *C. ljungdahlii*. The importance of PLA for the activities of crucial enzymes in product synthetic pathways and the regulatory activity of Rex was revealed. These findings expand our understanding of the metabolic regulation of product synthesis in autotrophic acetogens. Moreover, the subsequent strain improvement achieved a more efficient synthesis of the target product.

To our knowledge, it still remains poorly understood at the molecular level how autotrophic clostridia regulate the carbon flux distribution in product synthesis; only temperature, pH, and redox potential have been found to play roles in this aspect (8, 21, 22). In saccharolytic clostridia (such as *C. acetobutylicum*), some TFs have been reported to directly regulate product synthesis and affect the yield of different products, including Spo0A, CsrA, CcpA, AbrB, Rex, and SpoIIE (18, 19, 23–27). Interestingly, the homologs of all these

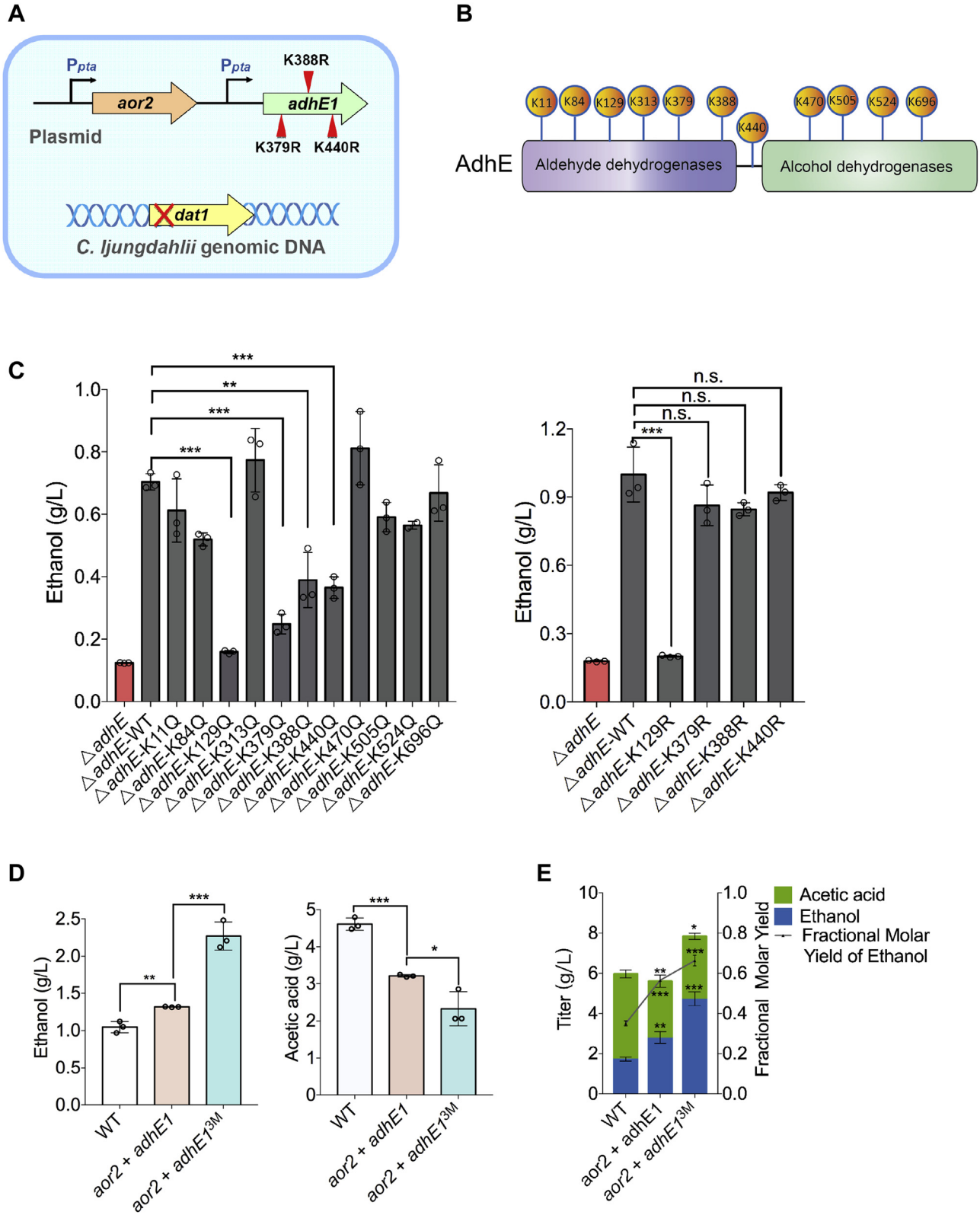

Figure 5. Improving the product synthesis pattern of *Clostridium ljungdahlii* by a modified module for *adhE1* expression. *A*, metabolic engineering strategies for *C. ljungdahlii*. *B*, acetylated lysine residues on AdhE1. *C*, identification of the key acetylation sites on AdhE1 by acetylation-mimicking mutations. The K129Q, K379Q, K388Q, and K440Q mutations led to significant loss in ethanol production. The K129R mutant greatly impaired ethanol formation. *D*, ethanol and acetic acid production of strains harboring the empty plasmid (WT) or the plasmid expressing *aor2* and *adhE1*, and *aor2* and *adhE1*^{3M} in gas fermentation. *E*, ethanol and acetic acid production of strains harboring the empty plasmid (WT) or the plasmid expressing *aor2* and *adhE1*^{3M} in gas fermentation with the addition of $CaCO_3$ (0.1% w/v) into the medium. The data are presented as mean ± SD (error bars; n = 3). Statistical analysis was performed using a two-tailed Student's *t* test. ***$p < 0.001$; **$p < 0.01$; *$p < 0.05$. AdhE1/2, bifunctional alcohol and aldehyde dehydrogenase; Aor1/2, aldehyde:ferredoxin oxidoreductase; Pta, phosphotransacetylase.

TFs can be found in autotrophic *C. ljungdahlii* (Table S4). However, considering the different product spectrum between saccharolytic and gas-fermenting *Clostridium* species, the action mechanisms of these TFs in *C. ljungdahlii* may be unique, which warrant further exploration.

The importance of posttranslational modifications in controlling crucial physiological and metabolic processes of autotrophic clostridia has not yet been recognized. Herein, the findings regarding the influence of PLA on the activities of Pta and AdhE1 as well as the regulator Rex in *C. ljungdahlii* revealed the physiological significance of PLA in these autotrophic acetogens. Although PLA often has relatively slight effects on enzyme activity, we found that it plays an important role in the regulation of product synthetic pathways in *C. ljungdahlii*. Pta, AdhE1, and Rex had relatively low acetylation status in the early stage, but this gradually increased with the extension of fermentation (Fig. 4), indicating that the major acetyltransferases in *C. ljungdahlii* play more critical roles in the later stage. The low acetylation levels of these key enzymes in the early stage may be because of the low supply of acetyl groups from acetyl-CoA or acetyl-phosphate at the beginning of gas fermentation, an energy-limited process.

To date, only very few transcriptional factors have been reported to be affected by PLA and then exhibit altered regulatory functions, including the *Saccharopolyspora erythraea* GlnR that regulates nitrogen metabolism (16), the hybrid sensor RcsC of the *Escherichia coli* two-component signal transduction system (17), and the global regulator CcpA in *C. ljungdahlii* (15). Rex is known as a TF capable of sensing the intracellular NADH/NAD^+ redox balance in bacteria (18, 28–32). The structures of the *Thermus aquaticus* Rex/NAD^+ and Rex/NADH revealed that NADH association could cause a dramatic conformational change that may alter the Rex binding to target DNAs, in which several highly conserved residues that are important for NADH/NAD^+ sensing were identified (29). The homology modeling results (Fig. S6) showed that the location of a key acetylated lysine residue, K17 (Fig. 3*E*), inside the *C. ljungdahlii* Rex was very close to the conserved domain responsible for DNA binding. Therefore, it can be speculated that the higher acetylation level of K17 may impair the Rex-DNA affinity, thereby decreasing the regulatory activity of Rex.

A detailed understanding of the regulatory mechanism of lysine acetylation on the synthesis of acetic acid and ethanol also provides a useful clue for improving the cellular performance of *C. ljungdahlii* in gas fermentation. In the metabolic engineering of industrial bacteria, the optimization of the transcription or translation efficiencies of target genes still represents the most widely used strategy. However, currently, the optimization of posttranslational modification is also an aspect that cannot be ignored. As lysine acetylation is crucial for the activities of some key enzymes and regulators related to product formation in *C. ljungdahlii*, the modulation of their acetylation levels should also be considered in genetic modification to achieve the desired synthetic ability of target products.

In summary, this study presents an unreported PLA-mediated cross-regulatory mechanism that controls the synthesis of acids and alcohols in autotrophic acetogens (Fig. 6), suggesting a new physiological role and application value of PLA in bacteria. In addition, many acetogens, including gut clostridia, are known to be the major human intestinal bacteria (33) and capable of producing various short-chain fatty acids and alcohols that contribute a lot to human intestinal health (34). Therefore, our work may also provide a new perspective regarding the importance of PLA in gut bacteria.

Experimental procedures

Bacterial strains, plasmids, media, and growth conditions

Escherichia coli strains DH5α and BL21(DE3) were used as the hosts for plasmid construction and protein expression. The cells were cultivated in an LB medium (35) supplemented with 12.5 μg/ml chloramphenicol or 100 μg/ml kanamycin when needed. The *C. ljungdahlii* strain DSM 13528 was incubated anaerobically at 37 °C in a YTF medium for inoculum preparation and a modified ATCC medium 1754 for gas fermentation ($CO–CO_2–H_2–N_2$; 56%/20%/9%/15%; pressurized to

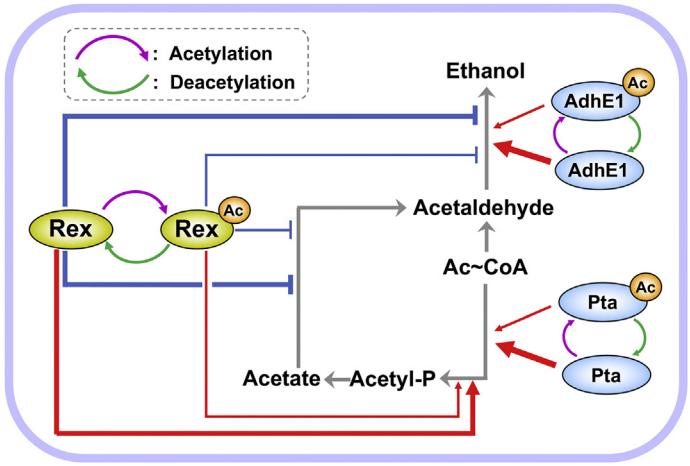

Figure 6. Lysine acetylation-mediated cross-regulatory mechanism to control product synthesis in *Clostridium ljungdahlii*. The *thick blue T-end lines* indicate stronger Rex-mediated transcriptional repression. The *thick red arrows* indicate stronger AdhE1/Pta-based catalytic activity and Rex-mediated transcriptional activation. AdhE1/2, bifunctional alcohol and aldehyde dehydrogenase; Pta, phosphotransacetylase.

0.2 MPa) (36). Thiamphenicol (5 μg/ml) was used when needed. All the strains used in this study are listed in Table S2.

Plasmid construction

All the primers used in this work are presented in Table S3. The plasmid pMTLcas-*ack* (for *ack* deletion) was constructed as follows: the plasmid pMTLcas (36) containing the *cas9* gene from *Streptococcus pyogenes* was treated with SalI and XhoI. Next, the sgRNA fragment was cloned through PCR-amplification using the plasmid pMTLcas as the template and the primers ack-gRNA-F/ack-gRNA-R. The two homologous arms (HAs) flanking the coding region of *ack* were amplified from *C. ljungdahlii* genomic DNA using the primers ackUparm-F/ackUparm-R or ackDownarm-F/ackDownarm-R and then linked to the sgRNA fragment through overlapping PCR using the primers ack-gRNA-F/ack Downarm-R, yielding the DNA fragment sgRNA-HA. Finally, the sgRNA-HA fragment and the aforementioned linear pMTLcas plasmid were assembled using a ClonExpress II one Step cloning kit (Vazyme Biotech Co, Ltd), yielding the plasmid pMTLcas-*ack*. The other plasmids (used for the deletion of *adhE2*, *aor1*, *aor2*, and *rex*) were constructed following the same steps; the only exception was that the HAs and sgRNA used were different.

The plasmid pMTL83151-P_{1440}-*dat1* (for *dat1* overexpression) was constructed as follows: the plasmid pMTL83151 was treated with BamHI and XbaI. Next, the promoter P_{1440} was cloned through PCR-amplification using *C. ljungdahlii* genomic DNA as the template and the primers P1440-F/P1440-R. The *dat1* gene was cloned through PCR-amplification using *C. ljungdahlii* genomic DNA as the template and the primers Dat1-1440-F/Dat1-1440-R. Finally, the aforementioned linear pMTL83151 plasmid, the promoter P_{1440}, and the *dat1* fragment were assembled using the ClonExpress MultiS One Step Cloning Kit (Vazyme Biotech Co, Ltd), yielding the plasmid pMTL83151-P_{1440}-*dat1*. The other gene overexpression plasmids were constructed following the same steps and using different primers.

Gene expression and protein purification

The CLJU_c12770, CLJU_c12780, CLJU_c16510, CLJU_c16520, CLJU_c20110, CLJU_c20210, and CLJU_c37250 genes, coding for Pta, Ack, AdhE1, AdhE2, Aor1, Aor2, and Rex, respectively, were expressed for the production of the corresponding proteins. For example, the *pta* gene was obtained through PCR amplification using the *C. ljungdahlii* genomic DNA as the template and the primers pET28a-Pta-F/pET28a-Pta-R. Then, the *pta* fragment and the linear plasmid pET28a, which was obtained by double digestion with NdeI and XhoI, were assembled using the ClonExpress II one Step cloning kit, yielding the target plasmid pET28a-Pta.

The other plasmids used for gene expression and protein purification were constructed in a similar manner, except that the coding regions of the genes were changed accordingly. The protein purification steps that followed were the same, as previously reported (25).

EMSA

The DNA probes used for EMSA were prepared as follows: the DNA fragments were obtained by PCR amplification using the *C. ljungdahlii* genomic DNA as the template and special primers containing a universal sequence (5′-AGCCAGTGGCGATAAG-3′) at the 5′ terminus. Next, the obtained DNA fragment was labeled with a Cy5 tag by PCR amplification using the universal primer containing Cy5. The yielded PCR products were further analyzed by agarose gel electrophoresis, recovered using a kit (catalog no. AP-GX-250; Axygen), and then used as probes for EMSAs. The following EMSA experiments were performed according to a previously reported protocol (25).

Real-time qRT-PCR

The *C. ljungdahlii* strain and its derivatives were grown anaerobically in a modified ATCC 1754 medium (36) using a CO-CO_2-H_2-N_2 mixture (56%-20%-9%-15%) at 37 °C. The cells were harvested at an absorbance (A_{600}) of 1.0. Total RNA was obtained by using a kit (catalog no. cw0581; CWBIO) and then treated by DNase I (TaKaRa) to eliminate DNA contained in the extracted samples. Here, a small quantity of the RNA treated by DNase I were used as the template for PCR amplification of the *rho* (CLJU_c02220) gene using the corresponding primers (Table S3), aiming to exclude the possibility of residual DNA in RNA samples. The RNA concentration was determined by using a NanoDrop spectrophotometer (Thermo Fisher Scientific). Then, cDNA was obtained *via* reverse transcription using a PrimeScript RT reagent kit (TaKaRa). The following real-time qPCR was carried out according to a previously reported protocol (15). The related primers are listed in Table S3. Here, the *rho* (CLJU_c02220) gene was used as the internal control (37).

Western blotting

The concentrations of the proteins were quantified by using Bradford Protein Assay kit (catalog no. C503041, Sangon Biotech, Co, Ltd). In brief, a standard curve for protein was first generated by absorbance measurements at 595 nm for a series of standard protein dilutions (bovine serum albumin; ranging from 10 to 200 μg/ml). The concentration of protein samples was then determined by reference to the standard curve. Next, the protein samples were separated through 12% SDS-PAGE and transferred to PVDF membranes for 40 to 60 min at 400 mA. The following procedures were carried out in the same manner, as previously reported (15).

The antibodies used in this work include anti-acetyl lysine antibody (ImmuneChem, ICP0380), anti-6×His tag Mouse mAb (Engibody Biotechnology, AT0025), Internal Controls-β-Tubulin (2H4) Mouse (Abmart, M30109S), HRP Goat Anti-Rabbit IgG (H + L) (ABclonal, AS014), and HRP Goat Anti-Mouse IgG (H + L) (ABclonal, AS003).

Enzyme activity assays

Pta

The assays were performed, as previously described (38) with slight modifications. In brief, a reaction mixture (1 ml) that contained 50 mM Tris–HCl (pH 8.0), 5 mM $MgCl_2$, 5 mM

KH_2PO_4, 0.18 mM acetyl-CoA, and 0.003 μM purified Pta protein was incubated at 37 °C for 40 s. Then, the reaction was terminated using 200 μl HCl (1 N). Next, a 200-μl reaction solution was mixed with a DTNB (0.1 mM) solution, and the mixture was incubated at room temperature for 2 min. The specific activity of Pta was measured by the changes in the spectrophotometric absorbance at A_{412}.

To test the influence of lysine acetylation on the enzymatic activity, the Pta protein was first treated *in vivo* by acetylase (At2), and then a certain amount of the mixture (equivalent to 0.003 μM Pta protein in the final reaction solution) was used for the following Pta activity assay. The same steps were used for investigating the influence of lysine acetylation on the activities of the other enzymes.

Ack

The enzyme activity assay of Ack was performed using a kit (BC3175, Solarbio) according to the manufacturer's instructions. In brief, the activity of Ack was examined by acetyl phosphate synthesis, which was further monitored through coupling with the oxidation reaction of NADH by employing pyruvate kinase and lactate dehydrogenase. The reaction mixture contained 20 mM of sodium-acetate, 50 mM of Hepes–NaOH (pH 7.5), 10 mM of $MgCl_2$, 1 mM of ATP, 0.25 mM of NADH, 5 mM of phosphoenolpyruvate, 20 units of lactate dehydrogenase, and 15 units of pyruvate kinase. The mixture was incubated at 25 °C and monitored every 10 s for 150 s. Finally, the specific activity of Ack was determined by measuring the change in absorbance at 340 nm caused by the oxidation of NADH on a DU730 spectrophotometer (Beckman Coulter).

AdhE1

The procedures were performed, as previously reported with slight modifications. All procedures were performed under anaerobic conditions. To measure the acetaldehyde dehydrogenase activity of AdhE1, we used a reaction mixture containing 50 mM Tris–HCl (PH 8.0), 0.1 mM NADH, 0.25 mM acetyl-CoA, 1 mM DTT, 5 μM $FeSO_4$, and appropriate amounts of AdhE1. To measure the alcohol dehydrogenase acetaldehyde activity of AdhE1, we used a reaction mixture containing 50 mM Tris–HCl (PH 8.0), 0.1 mM NADH, 10 mM acetaldehyde, 1 mM DTT, 5 μM $FeSO_4$, and appropriate amounts of AdhE1. The mixture was incubated at 37 °C, and the enzymatic activities were measured by the changes in the spectrophotometric absorbance values at A_{340} (39).

Aor2

The procedures were performed as previously reported with slight modifications. All procedures were performed under anaerobic conditions. The reaction mixture contained 50 mM Tris–HCl (PH 8.0), 0.6 mM methyl viologen, 0.6 mM sodium dithionite, 10 μM acetate, and appropriate amounts of Aor2. The mixture was incubated at 37 °C, and the enzymatic activities were measured by the changes in the spectrophotometric absorbance values at A_{600} (40, 41).

In vitro *acetylation and deacetylation assays*

In vitro acetylation assays were performed, as previously reported (15) with slight modifications. In brief, a 60-μl reaction system was constructed by mixing 50 mM Tris–HCl (pH 8.0), 2 μM of the target protein, 6 μM acetyltransferase (At2), 0.2 mM acetyl-CoA, and 5% glycerol, and then incubated at 37 °C for 3 h. Next, the mixture was divided into two aliquots for Western blot analysis and acetylation activity assay. Anti-acetyl lysine antibody (Cat# ICP0380) was purchased from ImmuneChem Pharmaceuticals Inc.

In vitro deacetylation assays were performed, as previously reported (15) with slight modifications. In brief, a 60-μl reaction system was constructed by mixing 50 mM Tris–HCl (PH 8.0), 2 μM of the target protein, 4 μM deacetylase (Dat1), 1 mM $MgCl_2$, 1 mM NAD^+, and 5% glycerol and then incubated at 37 °C for 3 h.

LC-MS/MS and data analysis

Chromatography was performed using the Easy nLC (Proxeon Biosystems, now Thermo Fisher Scientific) at a flow rate of 300 nl/min. The column was the C18 nanoViper (100-μm inner diameter, 200 mm length, Thermo Scientific). A 60-min gradient was used. Solvent A was water with 0.1% formic acid, and solvent B was acetonitrile with 0.1% formic acid. Peptides were separated with a gradient from 0% to 35% of solvent B over 50 min, 35% to 100% in 5 min, and climbing to 100% then holding at 100% for the last 5 min.

Peptides were introduced into a Q Exactive mass spectrometer (Thermo Scientific). The mass spectrometry survey scan was performed in positive ion mode with a resolution of 70,000 at 200 m/z, automatic gain control of 1E6, maximum fill time of 50 ms, dynamic exclusion duration of 60 s, and a scan range of 300 to 1800 m/z. Resolution for HCD spectra was set to 17,500 at 200 m/z, and isolation width was 2 m/z. Normalized collision energy was 30 eV and the underfill ratio, which specifies the minimum percentage of the target value likely to be reached at maximum fill time, was defined as 0.1%. The instrument was run with peptide recognition mode enabled. Mass spectrometry/MS spectra data were searched using Mascot 2.2 against the *C. ljungdahlii* database concatenated with reverse decoy database. Carboxamidomethyl was the fixed modification, with oxidation (Met) and acetyl (Lys) as dynamic modifications. The parameters were as follows: max missed cleavages of 2, peptide mass tolerance of 20 ppm, fragment mass tolerance of 0.1 Da, cleavage enzyme of trypsin, and the filter of score ≥20.

Fermentation

The inoculum preparation and gas fermentation of *C. ljungdahlii* were performed anaerobically in YTF and modified ATCC medium 1754, respectively, in which thiamphenicol (5 μg/ml) was added when needed. The detailed manipulations were similar to those previously described (36).

Analytical method

The growth of *C. ljungdahlii* was measured according to the absorbance of the culture at A_{600} using a spectrophotometer (DU730, Beckman Coulter). The concentrations of acetic acid and ethanol were measured according to previously described methods (36), using a 7890A gas chromatograph (Agilent) equipped with a flame ionization detector (Agilent) and a capillary column (Alltech ECTM-Wax).

Data availability

The raw mass spectrometry data have been deposited in iProX (www.iprox.org) with accession number of IPX0003487000, IPX0003648000, and IPX0003486000. Other relevant data supporting the findings of this research are available in the article and the Supplementary Information. In addition, datasets generated and analyzed in the study are available from the corresponding author upon reasonable requests.

Supporting information—This article contains supporting information.

Acknowledgments—This work was supported by the National Natural Science Foundation of China (31921006, 31630003), the National Key R&D Program of China (2018YFA0901500), the DNL Cooperation Fund, CAS (DNL202013), and Tianjin Synthetic Biotechnology Innovation Capacity Improvement Project (TSBICIP-KJGG-016-01).

Author contributions—Y. L. and Z. Z. investigation; Y. L., W. J., and Y. G. writing–original draft; W. J. and Y. G. validation; W. J. and Y. G. conceptualization; W. J. and Y. G. supervision; W. J. and Y. G. project administration; W. J. and Y. G. funding acquisition.

Conflict of interest—The authors declare that they have no conflicts of interest with the contents of this article.

Abbreviations—The abbreviations used are: HAs, homologous arms; PLA, Protein Lysine acetylation; TFs, transcription factors.

References

1. Yang, Y., Nie, X., Jiang, Y., Yang, C., Gu, Y., and Jiang, W. (2018) Metabolic regulation in solventogenic clostridia: Regulators, mechanisms and engineering. *Biotechnol. Adv.* **36**, 905–914
2. Kasubuchi, M., Hasegawa, S., Hiramatsu, T., Ichimura, A., and Kimura, I. (2015) Dietary gut microbial metabolites, short-chain fatty acids, and host metabolic regulation. *Nutrients* **7**, 2839–2849
3. Amador-Noguez, D., Brasg, I. A., Feng, X. J., Roquet, N., and Rabinowitz, J. D. (2011) Metabolome remodeling during the acidogenic-solventogenic transition in *Clostridium acetobutylicum*. *Appl. Environ. Microbiol.* **77**, 7984–7997
4. Ragsdale, S. W., and Pierce, E. (2008) Acetogenesis and the Wood-Ljungdahl pathway of CO_2 fixation. *Biochim. Biophys. Acta* **1784**, 1873–1898
5. Koepke, M., Held, C., Hujer, S., Liesegang, H., Wiezer, A., Wollherr, A., Ehrenreich, A., Liebl, W., Gottschalk, G., and Duerre, P. (2010) *Clostridium ljungdahlii* represents a microbial production platform based on syngas. *Proc. Natl. Acad. Sci. U. S. A.* **107**, 13087–13092
6. Zhang, L., Zhao, R., Jia, D., Jiang, W., and Gu, Y. (2020) Engineering *Clostridium ljungdahlii* as the gas-fermenting cell factory for the production of biofuels and biochemicals. *Curr. Opin. Chem. Biol.* **59**, 54–61
7. Furdui, C., and Ragsdale, S. W. (2000) The role of pyruvate ferredoxin oxidoreductase in pyruvate synthesis during autotrophic growth by the Wood-Ljungdahl pathway. *J. Biol. Chem.* **275**, 28494–28499
8. Ramió-Pujol, S., Ganigué, R., Bañeras, L., and Colprim, J. (2015) Incubation at 25 °C prevents acid crash and enhances alcohol production in *Clostridium carboxidivorans* P7. *Bioresour. Technol.* **192**, 296–303
9. Shen, S., Gu, Y., Chai, C., Jiang, W., Zhuang, Y., and Wang, Y. (2017) Enhanced alcohol titre and ratio in carbon monoxide-rich off-gas fermentation of *Clostridium carboxidivorans* through combination of trace metals optimization with variable-temperature cultivation. *Bioresour. Technol.* **239**, 236–243
10. Ammam, F., Tremblay, P. L., Lizak, D. M., and Zhang, T. (2016) Effect of tungstate on acetate and ethanol production by the electrosynthetic bacterium *Sporomusa ovata*. *Biotechnol. Biofuels* **9**, 163
11. Valgepea, K., Loi, K. Q., Behrendorff, J. B., Lemgruber, R. S. P., Plan, M., Hodson, M. P., Köpke, M., Nielsen, L. K., and Marcellin, E. (2017) Arginine deiminase pathway provides ATP and boosts growth of the gas-fermenting acetogen *Clostridium autoethanogenum*. *Metab. Eng.* **41**, 202–211
12. Zhao, S., Xu, W., Jiang, W., Yu, W., Lin, Y., Zhang, T., Yao, J., Zhou, L., Zeng, Y., Li, H., Li, Y., Shi, J., An, W., Hancock, S. M., He, F., *et al.* (2010) Regulation of cellular metabolism by protein lysine acetylation. *Science* **327**, 1000–1004
13. Gordenin, D. A., Gong, F., Chiu, L.-Y., and Miller, K. M. (2016) Acetylation reader proteins: Linking acetylation signaling to genome maintenance and cancer. *PLoS Genet.* **12**, e1006272
14. Yang, X.-J., and Seto, E. (2008) Lysine acetylation: Codified crosstalk with other posttranslational modifications. *Mol. Cell* **31**, 449–461
15. Zhang, L., Liu, Y., Zhao, R., Zhang, C., Jiang, W., and Gu, Y. (2020) Interactive regulation of formate dehydrogenase during CO_2 fixation in gas-fermenting bacteria. *mBio* **11**, e00650-20
16. You, D., Yin, B.-C., Li, Z.-H., Zhou, Y., Yu, W.-B., Zuo, P., and Ye, B.-C. (2016) Sirtuin-dependent reversible lysine acetylation of glutamine synthetases reveals an autofeedback loop in nitrogen metabolism. *Proc. Natl. Acad. Sci. U. S. A.* **113**, 6653–6658
17. Hu, L. I., Chi, B. K., Kuhn, M. L., Filippova, E. V., Walker-Peddakotla, A. J., Bäsell, K., Becher, D., Anderson, W. F., Antelmann, H., and Wolfe, A. J. (2013) Acetylation of the response regulator RcsB controls transcription from a small RNA promoter. *J. Bacteriol.* **195**, 4174–4186
18. Zhang, L., Nie, X., Ravcheev, D. A., Rodionov, D. A., Sheng, J., Gu, Y., Yang, S., Jiang, W., and Yang, C. (2014) Redox-responsive repressor Rex modulates alcohol production and oxidative stress tolerance in *Clostridium acetobutylicum*. *J. Bacteriol.* **196**, 3949–3963
19. Scotcher, M. C., Rudolph, F. B., and Bennett, G. N. (2005) Expression of abrB310 and sinR, and effects of decreased abrB310 expression on the transition from acidogenesis to solventogenesis, in *Clostridium acetobutylicum* ATCC 824. *Appl. Environ. Microbiol.* **71**, 1987–1995
20. Zhang, C., Nie, X., Zhang, H., Wu, Y., He, H., Yang, C., Jiang, W., and Gu, Y. (2021) Functional dissection and modulation of the BirA protein for improved autotrophic growth of gas-fermenting *Clostridium ljungdahlii*. *Microb. Biotechnol.* **14**, 2072–2089
21. Yang, X., Tu, M., Xie, R., Adhikari, S., and Tong, Z. (2013) A comparison of three pH control methods for revealing effects of undissociated butyric acid on specific butanol production rate in batch fermentation of *Clostridium acetobutylicum*. *AMB Express* **3**, 3
22. Wang, S., Zhu, Y., Zhang, Y., and Li, Y. (2012) Controlling the oxidoreduction potential of the culture of *Clostridium acetobutylicum* leads to an earlier initiation of solventogenesis, thus increasing solvent productivity. *Appl. Microbiol. Biotechnol.* **93**, 1021–1030
23. Harris, L. M., Welker, N. E., and Papoutsakis, E. T. (2002) Northern, morphological, and fermentation analysis of *spo0A* inactivation and overexpression in *Clostridium acetobutylicum* ATCC 824. *J. Bacteriol.* **184**, 3586–3597
24. Tan, Y., Liu, Z.-Y., Liu, Z., Zheng, H.-J., and Li, F.-L. (2015) Comparative transcriptome analysis between *csrA*-disruption *Clostridium acetobutylicum* and its parent strain. *Mol. Biosyst.* **11**, 1434–1442
25. Ren, C., Gu, Y., Wu, Y., Zhang, W., Yang, C., Yang, S., and Jiang, W. (2012) Pleiotropic functions of catabolite control protein CcpA in butanol-producing *Clostridium acetobutylicum*. *BMC Genomics* **13**, 349

26. Yang, Y., Zhang, L., Huang, H., Yang, C., Yang, S., Gu, Y., and Jiang, W. (2017) A flexible binding site architecture provides new insights into CcpA global regulation in Gram-positive bacteria. *mBio* **8**, e02004-16
27. Scotcher, M. C., and Bennett, G. N. (2005) SpoIIE regulates sporulation but does not directly affect solventogenesis in *Clostridium acetobutylicum* ATCC 824. *J. Bacteriol.* **187**, 1930–1936
28. Brekasis, D., and Paget, M. S. (2003) A novel sensor of NADH/NAD+ redox poise in *Streptomyces coelicolor* A3(2). *EMBO J.* **22**, 4856–4865
29. McLaughlin, K. J., Strain-Damere, C. M., Xie, K., Brekasis, D., Soares, A. S., Paget, M. S. B., and Kielkopf, C. L. (2010) Structural basis for NADH/NAD^+ redox sensing by a Rex family repressor. *Mol. Cell* **38**, 563–575
30. Wietzke, M., and Bahl, H. (2012) The redox-sensing protein Rex, a transcriptional regulator of solventogenesis in *Clostridium acetobutylicum*. *Appl. Microbiol. Biotechnol.* **96**, 749–761
31. Marshall, D. D., Sadykov, M. R., Thomas, V. C., Bayles, K. W., and Powers, R. (2016) Redox imbalance underlies the fitness defect associated with inactivation of the Pta-AckA pathway in *Staphylococcus aureus*. *J. Proteome Res.* **15**, 1205–1212
32. Alsaker, K. V., Spitzer, T. R., and Papoutsakis, E. T. (2004) Transcriptional analysis of *spo0A* overexpression in *Clostridium acetobutylicum* and its effect on the cell's response to butanol stress. *J. Bacteriol.* **186**, 1959–1971
33. Li, J., Jia, H., Cai, X., Zhong, H., Feng, Q., Sunagawa, S., Arumugam, M., Kultima, J. R., Prifti, E., Nielsen, T., Juncker, A. S., Manichanh, C., Chen, B., Zhang, W., Levenez, F., *et al*. (2014) An integrated catalog of reference genes in the human gut microbiome. *Nat. Biotechnol.* **32**, 834–841
34. Flint, H. J., Bayer, E. A., Rincon, M. T., Lamed, R., and White, B. A. (2008) Polysaccharide utilization by gut bacteria: Potential for new insights from genomic analysis. *Nat. Rev. Microbiol.* **6**, 121–131
35. Bertani, G. (2004) Lysogeny at mid-twentieth century: P1, P2, and other experimental systems. *J. Bacteriol.* **186**, 595–600
36. Huang, H., Chai, C., Li, N., Rowe, P., Minton, N. P., Yang, S., Jiang, W., and Gu, Y. (2016) CRISPR/Cas9-based efficient genome editing in *Clostridium ljungdahlii*, an autotrophic gas-fermenting bacterium. *ACS Synth. Biol.* **5**, 1355–1361
37. Zhao, R., Liu, Y., Zhang, H., Chai, C., Wang, J., Jiang, W., and Gu, Y. (2019) CRISPR-Cas12a-mediated gene deletion and regulation in *Clostridium ljungdahlii* and its application in carbon flux redirection in synthesis gas fermentation. *ACS Synth. Biol.* **8**, 2270–2279
38. Bock, A. K., Glasemacher, J., Schmidt, R., and Schonheit, P. (1999) Purification and characterization of two extremely thermostable enzymes, phosphate acetyltransferase and acetate kinase, from the hyperthermophilic eubacterium *Thermotoga maritima*. *J. Bacteriol.* **181**, 1861–1867
39. Zheng, T., Olson, D. G., Tian, L., Bomble, Y. J., Himmel, M. E., Lo, J., Hon, S., Shaw, A. J., van Dijken, J. P., and Lynd, L. R. (2015) Cofactor specificity of the bifunctional alcohol and aldehyde dehydrogenase (AdhE) in wild-type and mutant *Clostridium thermocellum* and *Thermoanaerobacterium saccharolyticum*. *J. Bacteriol.* **197**, 2610–2619
40. Whitham, J. M., Tirado-Acevedo, O., Chinn, M. S., Pawlak, J. J., and Grunden, A. M. (2015) Metabolic response of *Clostridium ljungdahlii* to oxygen exposure. *Appl. Environ. Microbiol.* **81**, 8379–8391
41. Heider, J., Ma, K., and Adams, M. W. W. (1995) Purification, characterization, and metabolic function of tungsten-containing aldehyde ferredoxin oxidoreductase from the hyperthermophilic and proteolytic archaeon *thermococcus* strain ES-1. *J. Bacteriol.* **177**, 4757–4764